

Novel transmission property of zero-index metamaterial waveguide doped with gain and lossy defects

Qionggan Zhu(朱琼干), Lichen Chai(柴立臣), and Hai Lu(路海)
Citation: Chin. Phys. B, 2023, 32 (**10**): 104215. DOI: 10.1088/1674-1056/acedf6
Journal homepage: http://cpb.iphy.ac.cn; http://iopscience.iop.org/cpb

What follows is a list of articles you may be interested in

Novel transmission property of zero-index metamaterial waveguide doped with gain and lossy defects

Qionggan Zhu(朱琼干), Lichen Chai(柴立臣), and Hai Lu(路海)
Chin. Phys. B, 2023, 32 (**10**): 104215. DOI: 10.1088/1674-1056/acedf6

Nonlinear perturbation of a high-order exceptional point: Skin discrete breathers and the hierarchical power-law scaling

Hui Jiang(江慧), Enhong Cheng(成恩宏), Ziyu Zhou(周子榆), and Li-Jun Lang(郎利君)
Chin. Phys. B, 2023, 32 (**8**): 084203. DOI: 10.1088/1674-1056/accb47

Fast population transfer with a superconducting qutrit via non-Hermitian shortcut to adiabaticity

Xin-Ping Dong(董新平), Zhi-Bo Feng(冯志波), Xiao-Jing Lu(路晓静), Ming Li(李明), and Zheng-Yin Zhao(赵正印)
Chin. Phys. B, 2023, 32 (**3**): 034201. DOI: 10.1088/1674-1056/ac8926

Anti-$\mathcal{PT}$-symmetric Kerr gyroscope

Huilai Zhang(张会来), Meiyu Peng(彭美瑜), Xun-Wei Xu(徐勋卫), and Hui Jing(景辉)
Chin. Phys. B, 2022, 31 (**1**): 014215. DOI: 10.1088/1674-1056/ac3988

Dissipative dynamics of an entangled three-qubit system via non-Hermitian Hamiltonian: Its correspondence with Markovian and non-Markovian regimes

M Rastegarzadeh and M K Tavassoly
Chin. Phys. B, 2021, 30 (**3**): 034205. DOI: 10.1088/1674-1056/abc2c3

Novel transmission property of zero-index metamaterial waveguide doped with gain and lossy defects

Qionggan Zhu(朱琼干)[1], Lichen Chai(柴立臣)[1], and Hai Lu(路海)[2,†]

[1] *Department of Science, Taiyuan Institute of Technology, Taiyuan* 030008, *China*
[2] *Engineering Laboratory for Optoelectronic Technology and Advanced Manufacturing, School of Physics, Henan Normal University, Xinxiang* 453007, *China*

(Received 6 June 2023; revised manuscript received 29 July 2023; accepted manuscript online 8 August 2023)

Taking inspiration from quantum parity–time (PT) symmetries that have gained immense popularity in the emerging fields of non- Hermitian optics and photonics, the interest of exploring more generalized gain-loss interactions is never seen down. In this paper we theoretically present new fantastic properties through a zero-index metamaterial (ZIM) waveguide loaded gain and loss defects. For the case of epsilon-and-mu-near-zero (EMNZ) based ZIM medium, electromagnetic (EM) waves are cumulative and the system behaves as an amplifier when the loss cavity coefficient is greater than the gain cavity coefficient. Conversely, when loss is less than gain, EM waves are dissipated and the system behaves as an attenuator. Moreover, our investigation is extended to non-Hermitian scenarios characterized by tailored distributions of gain and loss in the epsilon-near-zero (ENZ) host medium. The transport effect in ZIM waveguide is amplified in one mode, while it is dissipative in the other mode, which breaks the common sense and its physic is analyzed by magnetic flux. That is which cavity has the smaller loss/gain coefficient, the larger its magnetic flux, which cavity dominates. This paper is of significant importance in the manipulation of electromagnetic waves and light amplification as well as the enhancement of matter interactions.

Keywords: zero-index metamaterial, non-Hermitian, gain-loss interaction, magnetic flux

PACS: 42.25.Bs, 41.20.Jb, 73.20.Mf **DOI:** 10.1088/1674-1056/acedf6

1. Introduction

Nowdays non-Hermitian optic prevails among researchers in related fields due to their hyperphysical applications such as communications and lasing.[1–3] The PT symmetry can be implemented in optical systems because the gain and loss are easy to realize experimentally. By introducing equal amounts of gain and loss into a material to ensure that the refractive index satisfies $n(x) = n^*(-x)$, a PT-symmetric optical system is formed. In such a system, two or more modes can merge and undergo a phase transition from real energy spectrum to complex energy spectrum at exceptional point (EP).[4] The PT symmetry not only provides additional spatial modulation in optical systems, but also brings about new physical effects, such as negative refraction,[5] asymmetric invisibility,[6] and splitting of bound states in the continuum (BICs) into two states with purely real energy: PT-BICs and threshold states.[7]

Zero-index metamaterial (ZIM) refers to material whose dielectric constant and magnetic permeability are both close to zero or one of them approaches to zero, *i.e.* epsilon-near-zero (ENZ) and magnetic permeability-near-zero (MNZ) materials. In the past decade, ZIM have been widely used in energy squeezing,[8] wavefront manipulation,[9,10] waveguide bending,[11] energy flow control,[12] full transmission and reflection and optical field enhancement[13,14] because of their quasi-static field distribution. In addition, waveguide systems based on ZIM can achieve BICs without geometric symmetry requirements, providing new ideas for studying BICs in disordered systems.[15] Usually, the realization of MNZ materials is difficult and their application frequency is low, making their application range extremely limited. In recent years, researchers have shifted their focus to utilizing ENZ materials to realize effective material parameters for ZIM systems, from the perspective of material implementation and broader application frequency range.[16,17] Using the concept of photon doping, ENZ media can achieve effective magnetic response in a wide range of parameter regions. It means that the effective material parameters of ZIM systems can be customized by doping macroscopic media objects. Regardless of the position, size and number of doping objects, the composite material structure is equivalent to a uniform system with constant refractive index distribution.[18,19]

Since Viet Cuong Nguyen *et al.*[20] realized full transmission and reflection of light based on ZIM waveguide loaded with defect structures more than a decade ago, many unusual optical phenomena have been generated on this platform based on ZIM's quasi-static and photon-doping effects.[21,22] In previous studies, the system was generally considered to be ideal with no losses, and gain was later introduced to compensate for unavoidable losses. In fact, the interplay between gain and loss may have far-reaching implications that extend well beyond the mere compensation. The concept of quantum PT symmetry has inspired new ideas. Non-Hermitian optics extends conventional real-parameter space modulation to

[†]Corresponding author. E-mail: luhai123@gmail.com

© 2023 Chinese Physical Society and IOP Publishing Ltd

the complex space, where losses are not necessarily regarded as harmful effects. In some cases, they facilitate the interaction between light and matter to produce abnormal phenomena. In the SPP waveguide bypass coupled cavity structure, the competing mechanism between loss and gain produces some counterintuitive effects.[23] The combination of ZIM's quasi-static characteristics and PT symmetry can also produce rich physical effects, opening up new ideas for light field control, such as PT-induced asymmetric transmission,[24] CPA laser modes,[25] PT symmetry suppression,[26] and perfect resonance transmission.[27]

To investigate the intricate mechanisms of interactions between loss and gain in complex systems more comprehensively, this paper focuses on a two-dimensional (2D) ZIM waveguide doped with two gain and loss defetcts as the research platform. The responses of the system under non-Hermitian regulation of loss and gain are investigated under two conditions: ZIM filling media are epsilon-and-mu-near-zero (EMNZ) and epsilon-near-zero (ENZ). Moreover, the physical mechanism of abnormal transmission characteristics of waveguide is explored from the perspective of the magnetic flux and fields locality. The new interaction rules between loss and gain under the background field are revealed to provide some theoretical guidance for the application of non-Hermitian optical physics.

2. Model building

The schematic diagram in Fig. 1 illustrates the structure of a 2D waveguide filled with a ZIM medium, featuring two dielectric cylinder defects doped within the ZIM. The upper defect embedded in the ZIM meduim is the lossy cavity and the below one is the gain cavity. The permittivities of media in two chambers are assumed to be $\varepsilon_{\rm d}-{\rm i}\gamma_{\rm l}$ and $\varepsilon_{\rm d}+{\rm i}\gamma_{\rm g}$ respectively. In general, the loss can be easily obtained by nature materials, but not easy for gain medium. The fitted gain can be induced by laser systems or nonlinear multiple-wave mixing through external pumping.[28,29] Additionally, we consider an electromagnetic (EM) wave with $\boldsymbol{H}_{\rm inc}=H_{\rm inc}\exp({\rm i}k_0x)$ incident from the left inside the waveguide, where $k_0=\omega/c$ is the wave vector and $\omega=2\pi f$ is the angular frequency of incident wave. The working frequency f is set to 15 GHz in our calculation. The $\boldsymbol{H}_{\rm inc}$ field is polarized in the $\boldsymbol{z}$ direction, and the $\boldsymbol{E}_{\rm inc}$ field is directed along the $\boldsymbol{y}$ axis.

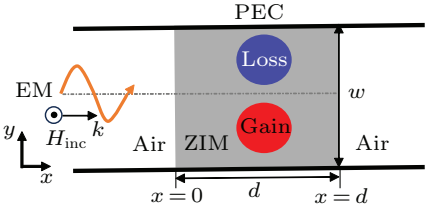


Fig. 1. Schematic diagram of the 2D air-ZIM-air waveguide loading gain and lossy cavities structure. The upper and lower boundaries are PECs. The width and length of the ZIM junction are w and d, their values are $w=60$ mm and $d=44$ mm, respectively. The radii of the gain and lossy cylinders are R_1 and R_2 ($R_1=R_2=8$ mm).

3. Theoretical derivation

To solve the transmission characteristics of the ZIM waveguide loaded defects, we can refer to Ref. [21]. By utilizing Maxwell's equation, the following Helmholtz equation is derived:

$$\begin{aligned}&\nabla^2\boldsymbol{H}_i+k_i^2\boldsymbol{H}_i=0,\\&\boldsymbol{H}_i|_{c_i}=H_0\boldsymbol{e}_{\boldsymbol{z}},\end{aligned}\tag{1}$$

where $\boldsymbol{H}_i$ ($i=1,2$) is the local magnetic field in the defect objects and H_0 is the quasi-static field of the ZIM background medium. The magnetic field and electric field inside each cylinder are obtained by the differential equation using the separation variable method. Then, by applying the Faraday–Maxwell equation and Stokes' theorem, we can further calculate transmission coefficient

$$\oint_{\partial C}\boldsymbol{E}\cdot{\rm d}\boldsymbol{l}+\sum_{i=1}^{N}\oint_{\partial C_i}\boldsymbol{E}_i\cdot{\rm d}\boldsymbol{l}=0,\tag{2}$$

where $\boldsymbol{E}$ is the electric field in the ZIM region and $\boldsymbol{E}_i$ is the electric field in each defect. Integral sign subscript ∂C is the boundary enclosing the whole ZIM region, and ∂C_i denotes the boundary of each defect, The transmittance coefficient t of the ZIM waveguide loading two-defect structure can be described as[15]

$$t=\frac{1}{1-({\rm i}\omega/2wH_0)\sum_{i=1}^{2}\oint\boldsymbol{A}_i{\rm d}\boldsymbol{l}},\tag{3}$$

where $\boldsymbol{A}_i$ ($i=1,2$) is the magnetic potential at the boundary of the two defective bodies. The magnetic flux of the defect cavity φ_i is written as

$$\varphi_{\rm i}=\oint\boldsymbol{A}_i{\rm d}\boldsymbol{l}=\frac{2\pi H_0}{\omega}\frac{{\rm J}_1(k_{\rm d}R_i)R_i}{{\rm J}_0(k_{\rm d}R_i)\sqrt{\varepsilon_{\rm d}}},\tag{4}$$

where $\rm J_0$ and $\rm J_1$ are the zero-order and first-order Bessel functions of the first kind respectively, $k_{\rm d}=\sqrt{\varepsilon_{\rm d}}\omega/c$ is the wave vector in the objects, c is the speed of light in vacuum.

3.1. Case I

When the two defect bodies are doped in the epsilon-and-mu-near-zero ZIM medium ($\varepsilon\approx0$, $\mu\approx0$), they can be regarded as two resonant chambers. The propagation properties of waveguide are independent of the defects' location in the ZIM. When two cavities introduce loss and gain respectively, the transmission coefficient can be written as

$$t=\frac{1}{1-\dfrac{{\rm i}\omega}{2wH_0}(\varphi_{\rm l}+\varphi_{\rm g})},\tag{5}$$

where $\varphi_{\rm l}$ and $\varphi_{\rm g}$ represents the magnetic flux of the loss cavity and the gain cavity respectively and they can be obtained by Eq. (4). We can observe that the transmission coefficient of the system is determined by the magnetic flux of both the loss and gain chambers.

3.2. Case II

When dealing with an ENZ-based ZIM host ($\varepsilon \approx 0$, $\mu = 1$), the transmission coefficient of the 2D waveguide with the lossy and gain dopants can be represented as follows:

$$t = \frac{1}{1 - \dfrac{\mathrm{i}\omega}{2wH_0}\left(\varphi_0 + \varphi_\mathrm{l} + \varphi_\mathrm{g}\right)}, \tag{6}$$

where the term $\varphi_0 = \mu H_0 (s - s_\mathrm{d})/c$ represents the magnetic flux of the quasi-static field H_0 through the ZIM region of waveguide, s denotes the entire area of ZIM and the defects area and s_d represents the area of two defects within the cavity. From Eq. (6), the transmittance coefficient of the waveguide is determined by the sum of the magnetic fluxes of both the loss and gain chambers plus ZIM. Therefore, the ENZ-based ZIM medium has characteristic of magnetic response due to non-zero magnetic flux, which provides a background field for the interaction of the loss cavity with the gain cavity.

4. Result and discussion

4.1. Case I

For the epsilon-and-mu-near-zero ZIM filling medium, due to the quasi-static field effect of ZIM, two defect bodies doped in the waveguide can be considered as two mutually-coupled, location-free resonant chambers.[15] When the defects are ideal and lossless, the mutual interference of the two chambers generates a resonance mode I, as shown in Fig. 2.

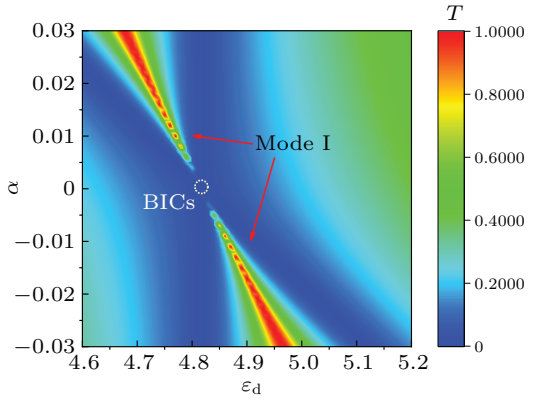


Fig. 2. The 2D map of the transmission coefficient as a function of the permittivity ε_d and the asymmetry parameter α. An ideal BICs occurs at $\alpha = 0$ and $\varepsilon_\mathrm{d} = 4.82$ (the white dotted circle).

The size difference between the two cavities radii is expressed by the asymmetry parameter α, where $\alpha = (R_2 - R_1)/R_1$. As the parameter α changes from nonzero to zero, mode I undergoes a transition from resonance mode to bound states in the continuum (BICs). If two resonant chambers introduce an equal amount of loss and gain separately ($\gamma_\mathrm{l} = \gamma_\mathrm{g}$), as shown in Fig. 3(a), the dissipation of the loss cavity and the amplification of the gain cavity are balanced. A transmission peak and a reflection dip appear around $\varepsilon_\mathrm{d} = 4.82$, and the sum of reflectance and transmission equals one. Therefore, the system remains generally balanced. However, when the loss and gain are not equal ($\gamma_\mathrm{l} \neq \gamma_\mathrm{g}$), the mutual competition between loss and gain leads to some counter-intuitive transmission characteristics in the waveguide. *i.e.* when $\gamma_\mathrm{l} > \gamma_\mathrm{g}$, as shown in Fig. 3(b), the sum of the reflectance and transmission are greater than one around $\varepsilon_\mathrm{d} = 4.82$, EM waves are cumulative and the system behaves as an amplifier. Conversely, when $\gamma_\mathrm{l} < \gamma_\mathrm{g}$, EM waves are dissipated and the system behaves as an attenuator.

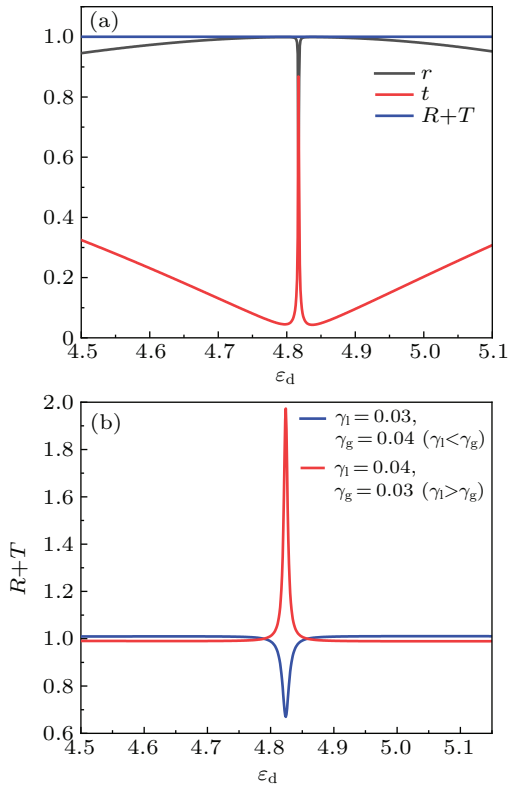


Fig. 3. The transmission coefficient t and reflection coefficient r as well as the sum of reflectivity R and transmittance T vary with the dielectric constant ε_d. (a) The case for the loss is equal to the gain ($\gamma_\mathrm{l} = \gamma_\mathrm{g} = 0.02$). (b) The sum of reflectivity R and transmittance T varies with the dielectric constant ε_d for the loss unequal to the gain. The permittivity and permeability of the ZIM host are $\varepsilon = \mu = 10^{-4}$.

The underlying physics of anomalous transmission of the system is revealed from the perspective of magnetic flux and field locality. Due to the introduction of loss and gain, the magnetic fluxes of defects become complex. For $\gamma_\mathrm{l} > \gamma_\mathrm{g}$, as depicted in Fig. 4(a), we have $\mathrm{Re}(\varphi_\mathrm{g}) > \mathrm{Re}(\varphi_\mathrm{l})$ and $-\mathrm{Im}(\varphi_\mathrm{g}) > \mathrm{Im}(\varphi_\mathrm{l})$ near the resonant transmission peak. Conversely, $\mathrm{Re}(\varphi_\mathrm{g}) < \mathrm{Re}(\varphi_\mathrm{l})$ and $-\mathrm{Im}(\varphi_\mathrm{g}) < \mathrm{Im}(\varphi_\mathrm{l})$ are observed in Fig. 4(b) for $\gamma_\mathrm{l} < \gamma_\mathrm{g}$. It shows that the larger coefficient of gain/loss cavity, the smaller real and imaginary parts of the magnetic flux. The difference of magnetic flux between two cylinders with gain and loss plays a crucial role in the counter-intuitive electromagnetic transmission through ZIMs waveguide. In which the cavity has the largest magnetic flux, and it dominates. Therefore, for the larger loss case, the magnitude of the complex-form magnetic flux of the gain cavity is

greater than that of the lossy cavity ($|\varphi_g| > |\varphi_l|$), as illustrated in Fig. 5(a). It is shown that the stronger field is localized in the gain cavity compared to that in the loss cavity. Consequently, the gain cavity plays a dominant role, and the system exhibits an amplified response. However, once the gain is greater, as shown in Fig. 5(b), the magnitude of the magnetic flux of the gain cavity translates to less than that of the loss cavity near the transmission peak ($|\varphi_g| < |\varphi_l|$), and the local field of the loss cavity becomes stronger. As a consequence, the loss cavity takes over, and the system exhibits a dissipated response.

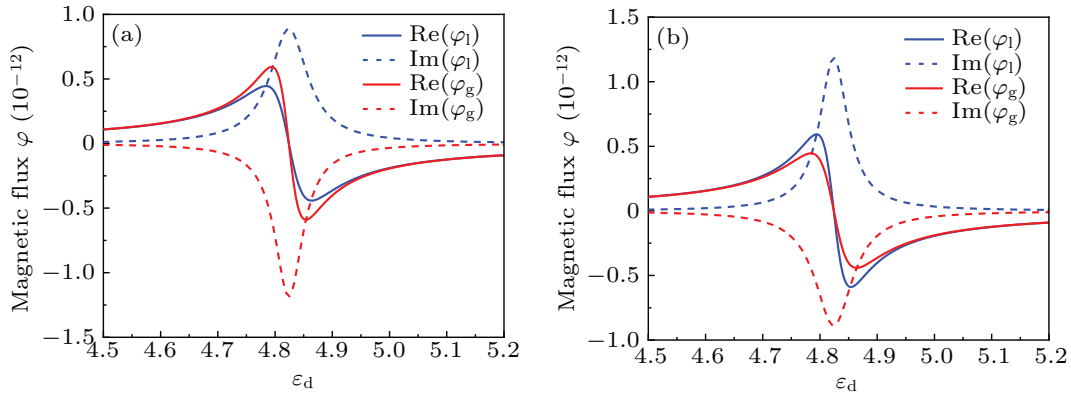


Fig. 4. The analytical φ_l and φ_g as a function of the permittivity ε_d. (a) Real part (solid red line) and imaginary part (dashed red line) of φ_g and real part (solid blue line) and imaginary part (dashed blue line) of φ_l for $\gamma_l = 0.04$, $\gamma_g = 0.03$. (b) Real part and imaginary part of φ_g and φ_l for $\gamma_l = 0.03$, $\gamma_g = 0.04$.

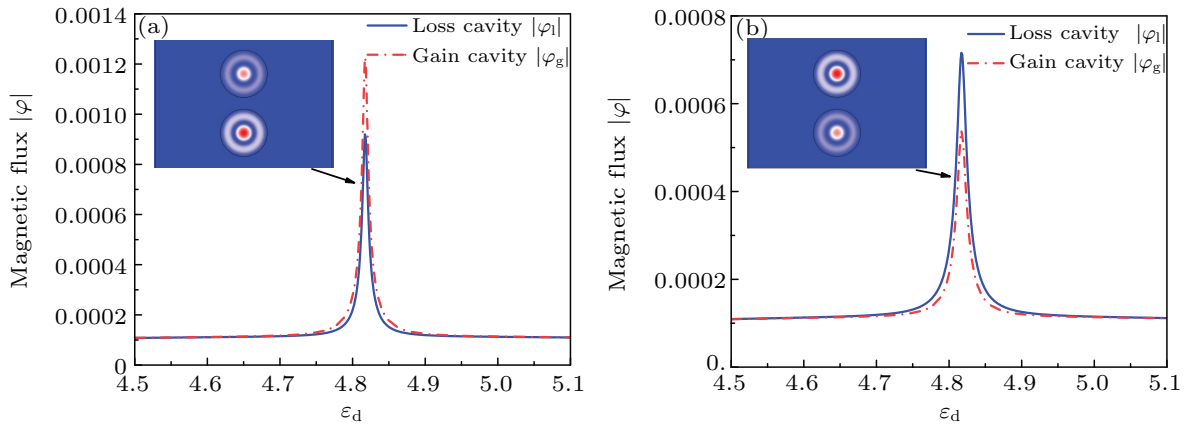


Fig. 5. Numerically calculated modulus of magnetic flux $|\varphi|$ varies with the dielectric constant ε_d for the EMNZ medium ($\varepsilon \approx 0$, $\mu \approx 0$). (a) The case for the larger loss ($\gamma_l = 0.04$, $\gamma_g = 0.03$). (b) The case for the larger gain ($\gamma_l = 0.03$, $\gamma_g = 0.04$). The simulated magnetic field modulus distribution in the ZIM region is shown respectively in the inset of panels (a) and (b). Numerical simulation is performed by using the finite element method software COMSOL Multiphysics. The numerical calculation of the magnetic flux modulus is obtained by the definition, that is, the integral of the magnetic field over the surface area ($|\varphi_i| = |\int_s \boldsymbol{B}_i \cdot \mathrm{d}\boldsymbol{s}|$).

4.2. Case II

For the ENZ-based host ($\mu \neq 0$) case, as shown in Fig. 6, the system supports two radiative monopole modes, and the mechanisms of the two modes are different. Mode I is similar to the mode I pattern in the case I, and it originates from the direct interference of the two chambers. As the asymmetric parameter α changes, there is also a conversion from BICs to resonance mode. Mode II is a Fano resonance which is based on the effect of the ZIM quasi-static field. It can be inferred from Eq. (6), magnetic field H_0 of the ZIM medium has a non-zero magnetic flux φ_0, hence mode II is produced by the two cavities seeing a resonant structure that interferes with the continuous quasi-static field H_0 in the medium. As the parameter α changes, resonance linewidth of mode II has no significant change.

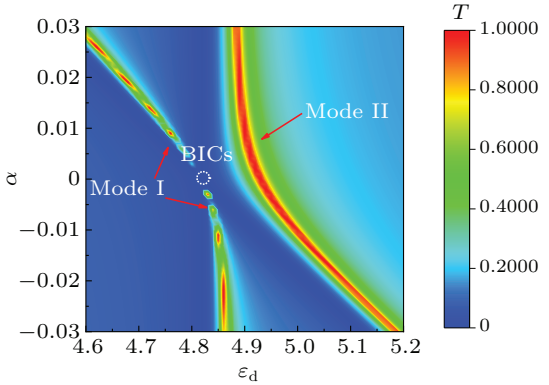


Fig. 6. The 2D map of the transmission coefficient as a function of the permittivity ε_d and the asymmetry parameter α.

When the equal loss and gain are introduced, as shown in Fig. 7, two transmission peaks appear in the reflection valleys around $\varepsilon_d = 4.82$ and $\varepsilon_d = 4.915$, respectively. The linewidth

of mode I is narrower than that of mode II. The sum of reflectance and transmission is equal to one. Under asymmetric control of loss and gain, the eccentric and different transport effects of waveguide corresponds to mode I and mode II.

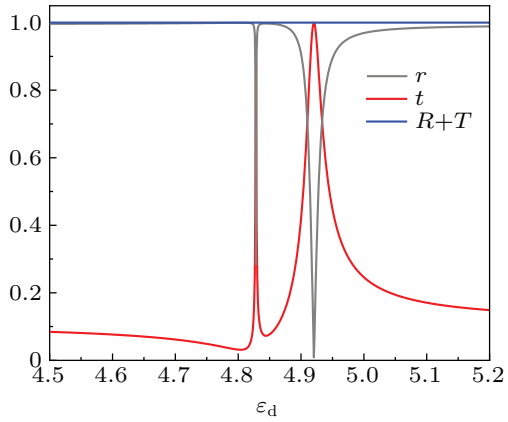


Fig. 7. The transmission coefficient t and reflection coefficient r as well as the sum of reflectivity R and transmittance T vary with the dielectric constant ε_d for the loss being equal to the gain ($\gamma_l = \gamma_g = 0.02$). The permittivity and permeability of the ZIM medium are $\varepsilon = 10^{-4}$ and $\mu = 1$.

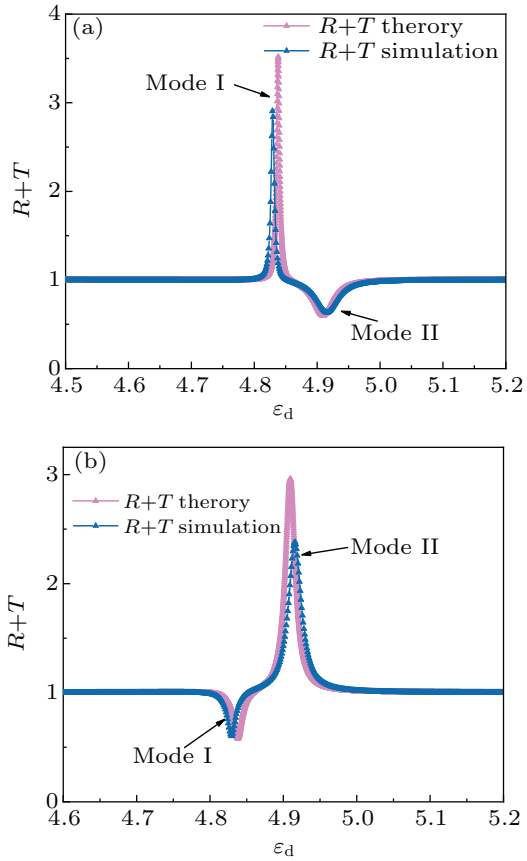


Fig. 8. The sum of reflectivity R and transmittance T varies with the dielectric constant ε_d. The solid pink line plus the triangle mark represents the theoretical calculation, and the blue–green solid line plus the triangle mark represents the simulation result. (a) The case for the loss is greater than the gain ($\gamma_l = 0.04$, $\gamma_g = 0.03$). (b) The case for the loss is less than the gain ($\gamma_l = 0.03$, $\gamma_g = 0.04$).

When $\gamma_l > \gamma_g$, as shown in Fig. 8(a), for mode I, the sum of reflectivity and reflectivity is less than 1, the system displays dissipative, while for mode II, the situation is just the opposite, the sum of transmittance and reflectivity is greater than 1, the system turns to be cumulative. When $\gamma_l < \gamma_g$, it can be seen in Fig. 8(b), for mode I, the sum of reflectivity and reflectivity is greater than 1, the system is cumulative, and for mode II, the sum of transmittance and reflectivity is less than 1, the system becomes dissipative.

Similarly, the mechanism behind it can be analyzed from the magnetic flux and local cavity field. For the ENZ case, the real and imaginary values of the magnetic flux φ_l and φ_g are identical in case I according to Eq. (4). Magnetic flux plotting is thus not repeated for the ENZ case. However, the analytical expression Eq. (4) presents the magnetic flux of individual defect, but it fails to describe the magnetic flux while the defects interact with the background field. The magnetic flux modulus of each cylinder was analyzed to further reveal the physics, with the simulated results shown in Fig. 9.

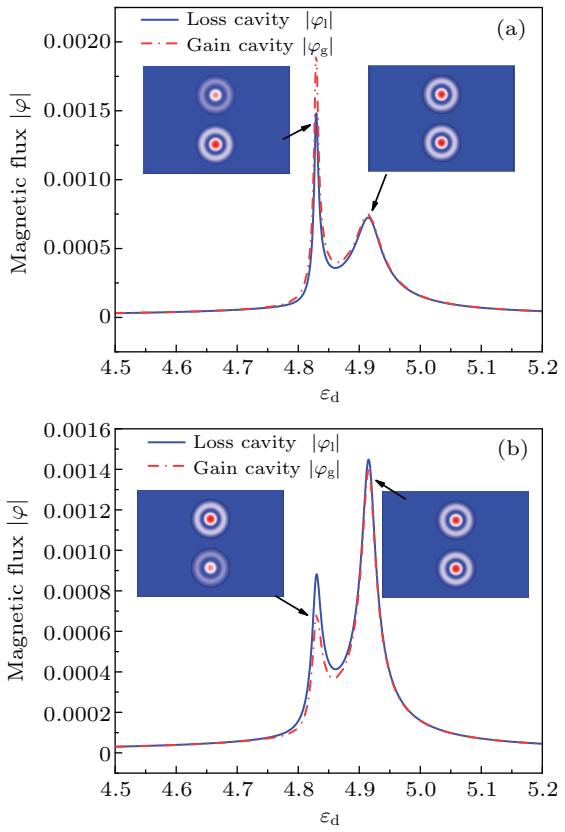


Fig. 9. Numerically calculated of the magnetic flux $|\varphi|$ varies with the dielectric constant ε_d for the ENZ medium ($\varepsilon \approx 0$, $\mu = 1$). (a) The case for the larger loss ($\gamma_l = 0.04$, $\gamma_g = 0.03$). (b) The case for the larger gain ($\gamma_l = 0.03$, $\gamma_g = 0.04$). Each inset in the graphs shows the simulated magnetic field modulus in the ZIM region at the resonant peak.

When $\gamma_l > \gamma_g$, for mode I, it can be seen from Fig. 9(a) that the magnetic flux and field local strength of the gain cavity are much larger than that of the lossy cavity, the amplification of the gain cavity is enhanced by the stronger field localization, therefore the gain cavity dominates, and the system is accumulated. The interaction between the loss cavity and the gain cavity is competitive for mode I. For mode II, the mag-

netic flux and local field strength in the gain cavity are close to that in the loss cavity, which is not enough to enhance the amplification of the gain cavity. The loss and gain cavities compensate each other. Because the loss cavity coefficient is larger, the overall performance of two cavities is lossy, and the system is dissipated. When $\gamma_l < \gamma_g$, as shown in Fig. 9(b), for mode I, the magnetic flux and field strength in the loss cavity are much larger than those in the gain cavity, which enhances the lossy effect of the loss cavity. The loss cavity thus dominates and the system is dissipated. For mode II, the magnetic flux of the loss cavity and the localized field strength are a little larger than those of the gain cavity, the effect of the total mutual compensation of the two chambers is the gain, so the system is cumulative.

5. Conclusion

The concept of photonic doping can be extended to non-Hermitian scenarios, where gain and loss are distributed in two dop bodies. The non-Hermitian interaction between loss and gain in complex systems is studied by using a 2D ZIM waveguide with loaded loss and gain defects as the platform. For the case of EMNZ-based ZIM medium, our results show that EM waves are cumulative and the system behaves as an amplifier under the resonant mode when the loss cavity coefficient is greater than the gain cavity coefficient. Conversely, when loss less than gain, EM waves are dissipated and the system behaves as an attenuator. For the case of ENZ host medium, the system supports two resonant modes based on the quasi-static field effect of ZIM. By tailoring the gain and loss, it is found that the responses of the system in these two modes are completely different. When the loss coefficient surpasses the gain, the system response becomes dissipative under one mode and accumulative under the other mode, and vice versa. The physical mechanism of the system's anomalies is explained from the perspective of magnetic flux and field locality. Our paper provides theoretical guidance for the application of light amplification and the gain–loss interaction of matter.

Acknowledgement

Project supported by Scientific and Technological Innovation Program of Higher Education Institutions in Shanxi Province, China (Grant No. 2021L554).

References

[1] Feng L, El-Ganainy R and Ge L 2017 *Nat. Photon.* **11** 752
[2] zdemir S K, Rotter S, Nori F and Yang L 2019 *Nat. Mater.* **18** 783
[3] Xu J F, Yang X B, Chen H H, *et al.* 2020 *Chin. Phys. B* **29** 064201
[4] Bender C M, Brody D C and Jones H F 2002 *Phys. Rev. Lett.* **89** 270401
[5] Fleury R, Sounas D L and Alù A 2014 *Phys. Rev. Lett.* **113** 023903
[6] Sounas D L, Fleury R and Alù A 2015 *Phys. Rev. Appl.* **4** 014005
[7] Song Q J, Dai S W, Han D Z, Zhang Z Q, Chan C T and Zi J 2021 *Chin. Phys. Lett.* **38** 084203
[8] Yi J, Z Pu Z and He S 2010 *Phys. Rev. B* **81** 085117
[9] Fu Y Y, Xu Y D and Chen H Y 2014 *Sci. Rep.* **4** 6428
[10] Huang X Q, Lai Y, Hang Z H, Zheng H H and Chan C T 2011 *Nat. Mater.* **10** 583
[11] Luo J, *et al.* 2012 *Appl. Phys. Lett.* **100** 221903
[12] Yang Y, Jia Z, Xu T, Luo J, Lai Y and Hang Z H 2019 *Appl. Phys. Lett.* **114** 161905
[13] Liberal I and Engheta N 2017 *Science* **358** 1540
[14] Liberal I and Engheta N 2017 *Nat. Photon.* **11** 149
[15] Zhou Q J, Fu Y Y, Huang L J, Wu Q N, Miroshnichenko A, Gao L and Xu Y D 2021 *Nat. Commun.* **12** 4390
[16] Niu X, Hu X, Chu S and Gong Q 2018 *Adv. Opt. Mater.* **6** 1701292
[17] Liberal I, Li Y and Engheta N 2018 *Nanophotonics* **7** 1117
[18] Liberal I, Mahmoud A M, Li Y, Edwards B and Engheta N 2017 *Science* **355** 1058
[19] Coppolaro M, Moccia M, Castaldi G, Engheta N and Galdi V 2020 *Proc. Acad. Natl. Sci. USA* **117** 13921
[20] Nguyen V C, Chen L and Halterman K 2010 *Phys. Rev. Lett.* **105** 233908
[21] Xu Y D and Chen H Y 2011 *Appl. Phys. Lett.* **98** 113501
[22] Fu Y Y, Zhang X J, Xu Y D and Chen H Y 2017 *J. Appl. Phys.* **121** 094503
[23] Zhu Q G, Tan W and Wang Z G 2014 *J. Phys.: Condens. Matter* **26** 255301
[24] Jin B and Argyropoulos C 2019 *Adv. Opt. Mater.* **7** 1901083
[25] Luo J, Liu B, Hang Z H and Lai Y 2018 *Laser & Photon. Rev.* **12** 1800001
[26] Fu Y Y, Xu Y D and Chen H Y 2016 *Opt. Express* **24** 1648
[27] Wang C, Zhou Q J, Jiang J H, Gao L and Xu Y D 2023 *Opt. Express* **31** 18487
[28] Rüter C E, Makris K G, El-Ganainy R, *et al.* 2010 *Nat. Phys.* **6** 192
[29] El-Ganainy R, Makris K G, Khajavikhan M, *et al.* 2018 *Nat. Phys.* **14** 11